

J. Electroanal. Chem., 319 (1991) 227–242
Elsevier Sequoia S.A., Lausanne
JEC 01760

Kinetics of oxidation and reduction of amorphous Ni + Co alloys

Keryn Lian * and V.I. Birss **

Chemistry Department, University of Calgary, Calgary, Alta. T2N 1N4 (Canada)

(Received 5 April 1991; in revised form 28 June 1991)

Abstract

The kinetics of the oxidation–reduction of hydrous oxide films formed electrochemically at an Ni + Co-based amorphous alloy in alkaline solutions display numerous similarities with many polymer-coated electrodes. In cyclic voltammetric experiments, the anodic response shows a strong dependence on the magnitude and the time spent at negative potentials, particularly in the case of relatively thick films, while the cathodic peak remains essentially unaffected by these variables. Potential step experiments show unusual maxima and peculiar anodic-to-cathodic charge ratios. These results have been explained in terms of ion/solvent injection/expulsion processes which take place during film oxidation–reduction and a disproportionation reaction which occurs within the oxide film under non-steady-state conditions.

INTRODUCTION

The rate of charge transport through electroactive films on electrode surfaces has been of interest for some time. This is due, in part, to their potential applications in such areas as electrocatalysis, energy conversion, electrochromism etc. [1–5]. In addition, the fundamental nature of the charge transport process through such films is also of importance, both in shedding light on the impact of film structure and composition on the kinetics and mechanisms involved and in optimizing film growth conditions to produce the most desirable electrode characteristics.

* Present address: Department of Metallurgy and Materials Science, University of Toronto, Toronto, Ont. M5S 1A4, Canada.

** To whom correspondence should be addressed.

In our previous papers [6,7], the electrochemical formation of hydrous oxide films at amorphous Ni + Co alloy electrodes was discussed. It was shown that numerous properties of these modified electrodes were very similar to systems in which electroactive polymers such as polyvinylferrocene [8–10], functionalized polystyrene [11,12], tetrathiofulvalene [12–14], polyaniline [15] etc. are coated on metal electrode surfaces. For example, the oxide film thickness at amorphous Ni + Co electrodes can be controllably varied from only a few monolayers to more than 500 nm during electrochemical growth [6]. The films appear to be gel-like in nature [6], which is evidence for the presence of solvent within the structure and for the likelihood of a flexible film backbone. The principal redox reaction of the oxide has been shown to involve the transport of both electrons and counter-ions; the reaction is also electrochromic. While these are all similar to the characteristics exhibited by numerous polymer-based systems, they also bear a strong resemblance to the features of hydrous oxide films formed at metals such as Ir [16–20] and Rh [21].

The focus of the present work concerns the kinetics of oxidation and reduction of these hydrous oxide films, as compared with polymer-modified and other metal oxide electrodes. It will be shown that film oxidation is quite different from reduction, indicative of a unique film structure and/or composition in each of these two states. Also, an unusual disproportionation reaction appears to take place during the rapid electrochemical reduction of these Ni + Co oxide films.

EXPERIMENTAL

The principal methods of investigation employed in this work were cyclic voltammetry (CV), chronoamperometry and chronocoulometry. The working electrode was an amorphous $\text{Ni}_{51}\text{Co}_{23}\text{Cr}_{10}\text{Mo}_7\text{Fe}_{5.5}\text{B}_{3.5}$ (wt.%) ribbon material, obtained from Allied-Signal Corporation and having a typical area of 0.1 cm^2 . Because of the difficulty of determining the true electrode area electrochemically, all current and charge densities are given with respect to the apparent electrode area. The counter-electrode was a large area Pt gauze and the reference electrode was the reversible hydrogen electrode (RHE), to which all potentials are referred. All experiments were carried out in 1 M NaOH solutions under an Ar atmosphere at room temperature.

A description of the instrumentation, cell, electrode preparation techniques, chemicals used and other general experimental methodologies employed have been given in detail in our previous papers [6,7].

RESULTS AND DISCUSSION

Cyclic voltammetric behavior

General features

In the first few cycles of potential of the amorphous Ni + Co alloy electrode in alkaline solutions, Cr (and possibly B, but not the other elements) dissolves from

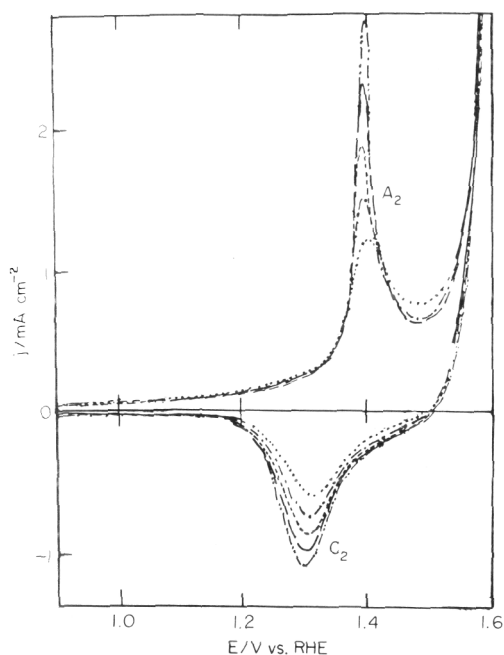
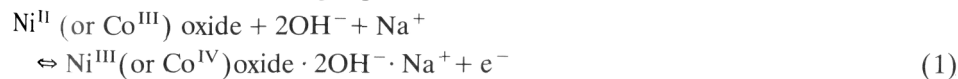


Fig. 1. CV response in third to seventh potential cycles of Ni + Co alloy in 1 M NaOH ($s = 100 \text{ mV s}^{-1}$).

an oxidized Cr-enriched surface region [6,7]. When the potential is then cycled (or pulsed) between critical upper (E_+) and lower (E_-) potential limits [6,7], similar to the requirements for the growth of hydrous oxide films at Ir [16,17], Rh [21], W [22] and polymers such as tetrathiofulvalene [12–14], the CV response shows a continuously increasing pair of redox peaks centered at ca. 1.35 V (Fig. 1), while the double-layer current remains constant and that due to the hydrogen evolution reaction (HER) decreases in magnitude.

The general appearance of the CV is most similar to that observed at polycrystalline Ni [1,2,23], although the peak shapes and oxide growth rate are quite different. The only electrochemical indicators of the presence of Co, which would have been expected to be electroactive in the potential range investigated, is the relative ease of electrochemical oxide growth and the pronounced electrochromism which can be seen vividly as the film thickens (Ar sputtering Auger electron spectroscopy (AES) analysis indicates Co presence at 30% [6]). Although AES analysis shows that Cr, Mo and Fe are at least partially retained in the oxide film [6], there are no electrochemical indications of their presence with continued cycling.

The process occurring in the principal pair of redox peaks in Fig. 1 has been ascribed [6] to the following representative reaction in NaOH solutions:



In Fig. 1, the oxide film is still thin after the last cycle shown, as indicated by the charge enhancement factor (CEF) of ca. 8. The CEF is determined from the ratio of the charge in the cathodic peak C_2 after a particular oxide growth period to that of a single monolayer of hydrous oxide film [6,7,24]. It can be seen that, contrary to the oxide film response at polycrystalline Ni and Co electrodes, a pronounced asymmetry is present between the anodic and cathodic peaks for the oxide formed at the amorphous alloy surface. The anodic peak is sharp and narrow, while the cathodic one is broader and smaller. These peak widths are not in agreement with the theoretical value of 90 mV for a one-electron transfer surface reaction.

According to Angerstein-Kozłowska *et al.* [25], who examined the electrochemical characteristics of monolayer films, the peak width is an almost linear function of the lateral interaction parameter g . Positive g values represent repulsive interactions between sites within the film, while negative g values imply that lateral attractive forces are present. This is similar to the suggestion by Peerce and Bard [9] for polymer films that attractive interactions yield sharp and narrow peaks, and vice versa for repulsive forces.

On the basis of reaction (1), the oxidized sites in the Ni + Co oxide film may be surrounded by excess OH^- ions (repulsive lateral interactions, broad CV peak), while the narrow anodic peak would then reflect less repulsive, more neutral environments around the electroactive sites in the reduced form of the film. This is equivalent to stating that the reduced film is more compact and highly cross-linked, while the oxidized film is more swollen and expanded.

Figure 2 demonstrates that, for a somewhat thicker film with CEF = 30, the asymmetry increases as the lower potential limit is extended to ca. 0.0 V. For thick films, the A_2 peak can be inhibited to such an extent that it is situated well within the potential range for the oxygen evolution reaction (OER).

Another variable which influences the A_2 peak shape and position is the potential sweep rate [6]. The faster the rate of perturbation, particularly to potentials near 0.0 V, the greater is the positive shift of A_2 and the more pronounced is the asymmetry between the anodic and cathodic response (Fig. 3). In the case of plasma polymerized vinylferrocene [8,10,26] and tetracyanoquinodimethane polymer films [27], both ions and solvent are injected during oxidation to maintain electroneutrality, causing swelling to an extent which depends on the type of solvent present, and vice versa during reduction. Therefore the oxidized and reduced forms of the film are thermodynamically different, involving different activities of the electroactive sites in the two forms of the film, and symmetrical peaks would not be expected.

Determination of apparent diffusion coefficient

As shown in Figs. 2 and 3, it is difficult to establish the peak current–sweep rate relationship reliably for peak A_2 , owing to the proximity of the OER and the variation in the peak characteristics with E_- , sweep rate etc., and therefore peak C_2 was examined for its sweep rate dependence. It has been shown previously [7] that a linear relationship is observed between peak current and sweep rate (up to

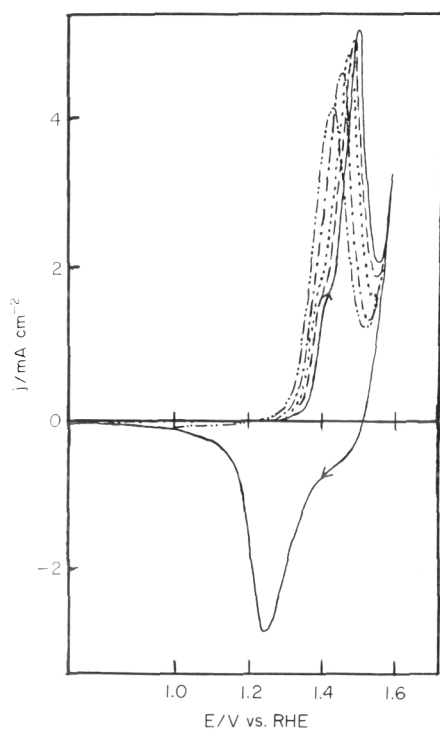


Fig. 2. Influence of lower potential limit on CV response at $s = 100 \text{ mV s}^{-1}$ of hydrous oxide film (CEF = 30): $E_- = 1.0 \text{ V}$ (- · - · -), 0.8 V (- - -), 0.6 V (· · · · ·), 0.4 V (- - -) and 0.2 V (— — —).

ca. 500 mV s^{-1}) for a thin hydrous oxide film (ca. 20 nm). However, in the case of thicker films, such a relationship is seen only at a relatively low sweep rate (Fig. 4, curve a), while at higher sweep rates an $s^{1/2}$ relationship is obtained (Fig. 4, curve b). The latter relationship has also been reported for numerous polymer-coated electrodes, and either electron hopping or associated ion transport can be considered to be rate limiting [10,11,28,29]. This interpretation of the observed kinetics could also apply to reaction (1), in which both ions and electrons are involved.

From the slope of the plot in curve b (Fig. 4), the apparent diffusion coefficient of the rate-limiting species during oxide reduction has been determined to be $1.9 \times 10^{-10} \text{ cm}^2 \text{ s}^{-1}$, using the semi-infinite linear diffusion equation [30]. This value is well within the range of 10^{-7} – $10^{-14} \text{ cm}^2 \text{ s}^{-1}$, obtained primarily for the oxidation step for many polymer electrode systems, and is also close to that obtained for Ni oxide oxidation in KOH solutions [31].

In many polymer studies, the rate-determining species is considered to be the counter-ion, and this may also be the case here. However, the rate of reduction of hydrous Ni + Co films may also be controlled by electron hopping if ion motion is relatively rapid, especially in the swollen condition of the film. In comparison, the coefficient obtained for the first oxidation–reduction step of hydrous Ir oxide in

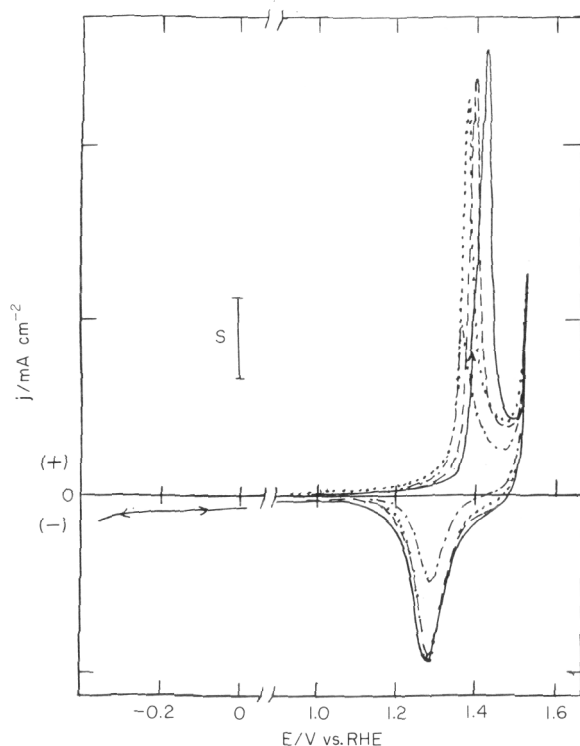


Fig. 3. Dependence of CV response (CEF = 18) on sweep rate: $s = 5 \text{ mV s}^{-1}$ (---), 10 mV s^{-1} (⋯⋯), 20 mV s^{-1} (- - -) and 50 mV s^{-1} (—); $S = 0.18 \text{ mA cm}^{-2}$ ($s = 5, 10 \text{ mV s}^{-1}$), 0.35 mA cm^{-2} ($s = 25 \text{ mV s}^{-1}$) and 0.7 mA cm^{-2} ($s = 50 \text{ mV s}^{-1}$).

alkaline solutions was $3 \times 10^{-9} \text{ cm}^2 \text{ s}^{-1}$ [20], attributed to electron hopping as the rate-controlling step.

Chronoamperometric behavior

General features and dependence of current maximum on experimental variables

The $j-t$ response of the hydrous Ni + Co oxide films to a potential step shows a number of unusual properties. Figure 5 demonstrates a series of transients obtained in response to a square wave potential program from 1.0 V to various E_+ values for an oxide film which is comparatively thin (CEF = 14). The response shown was virtually unchanged when IR compensation was used. At an E_+ value of 1.35 V (---), an apparently exponential decay of the anodic and cathodic currents was observed. At $E_+ = 1.38 \text{ V}$ (—), an abnormal anodic current maximum is seen, while when E_+ is increased further, the current maximum is still larger and appears at shorter times. At $E_+ = 1.45 \text{ V}$, a more typical exponentially decaying anodic transient is seen again. In each case, the cathodic $j-t$

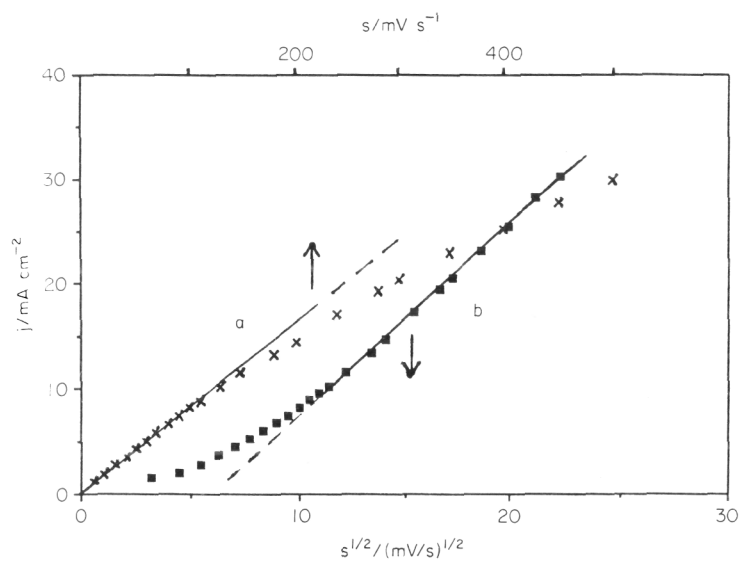


Fig. 4. Dependence of peak current density of C_2 on s (curve a) and $s^{1/2}$ (curve b) for oxide film with CEF = 97.

response has a more normal appearance, although there is a very important and marked difference in the anodic and cathodic charges passed (discussed in detail below).

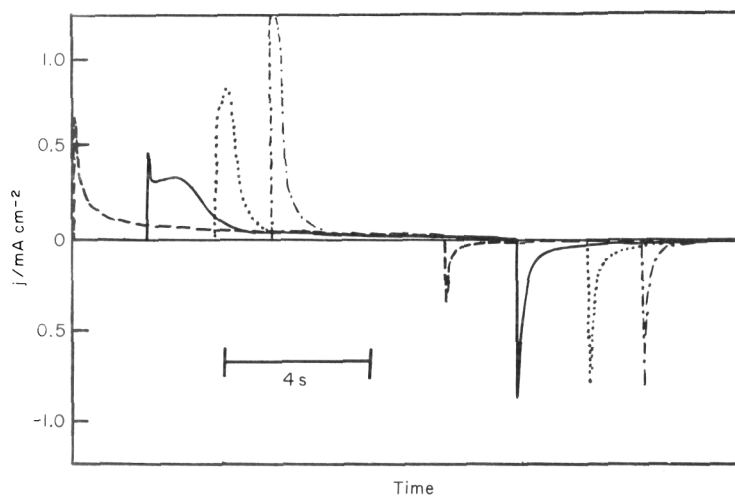


Fig. 5. $j-t$ response to potential steps from 1.0 V to $E_+ = 1.35$ V (---), 1.38 V (—), 1.40 V (····) and 1.45 V (-·-·).

In similar experiments carried out with electrochemically oxidized polycrystalline Ni and Co electrodes, anodic current maxima and differences in anodic and cathodic charges were never observed. Also, when electrochemically oxidized coprecipitated Ni + Co electrodes were subjected to the same tests [32], the peculiar behavior shown in Fig. 5 was not obtained.

Current maxima similar to those in Fig. 5 have been reported for a number of polymer-modified electrodes which require ion injection during oxidation [8,11,12]. In some of these studies, the anodic peak was considered to be related to a potential-dependent film resistance to ion and solvent flow. When E_+ is insufficient to overcome this resistance, film oxidation cannot be initiated rapidly. A certain amount of time and a critical internal concentration of ions and solvent is required to "break-in" the film, resulting in a resistance drop [8,12]. The cathodic $j-t$ response does not show such a peak, as the film is saturated with ions and solvent in the oxidized state so that the film resistance is low.

Film resistance prior to oxidation may also be related to poor electronic conductivity of the reduced form of the film. In this case, the "break-in" phenomenon could reflect an initially slow conversion of the film from a poor to a better electronic conductor. This interpretation may have some bearing on these Ni + Co oxide films, as Co^{III} , Ni^{II} and Ni^{III} oxides are all known to be poor electronic conductors relative to Co^{IV} and Ni^{IV} oxides [33].

Current maxima in $j-t$ transients can also imply that a nucleation process has occurred [34,35]. Using the above interpretations, it could be argued that, once oxidation commences, the increasing conductivity (either electronic or ionic) within the film catalyzes its further oxidation. This is similar to a nucleation process, in that the reaction will accelerate as it progresses until all the sites have been consumed, and therefore a current maximum would be predicted.

The shape of the $j-t$ transients for these oxidized amorphous alloy electrodes is also very dependent on E_- . Figure 6 shows that, at more negative E_- , the $j-t$ maximum appears at longer times. This is consistent with the results obtained in the CV experiments (e.g. Fig. 2), in which the negative extension of E_- causes the A_2 peak to shift positively, reflecting an increased inhibition to oxidation, while the peak width decreases, indicative of the catalytic nature of the process once it commences. Similar results have again been obtained with various polymer-coated electrodes [9,11,12] and have been interpreted in terms of the loss of ions/solvent from the film at negative potentials, causing the subsequent oxidation step to be more difficult.

It is of interest that for $E_- \geq 1.24$ V a smooth anodic current decay is seen (Fig. 7, ---) even for $E_+ \approx 1.37$ V when the abnormal current maximum is usually seen. When $E_- = 1.0$ V (Fig. 7, —), the anodic transient shows an incipient maximum at short times. The absence of the peak when E_- is sufficiently positive may indicate that insufficient time is available for complete ion/solvent expulsion (reaction (1)) or that the film is not completely reduced, thereby maintaining sufficient electronic conductivity to ease the subsequent oxidation process. This

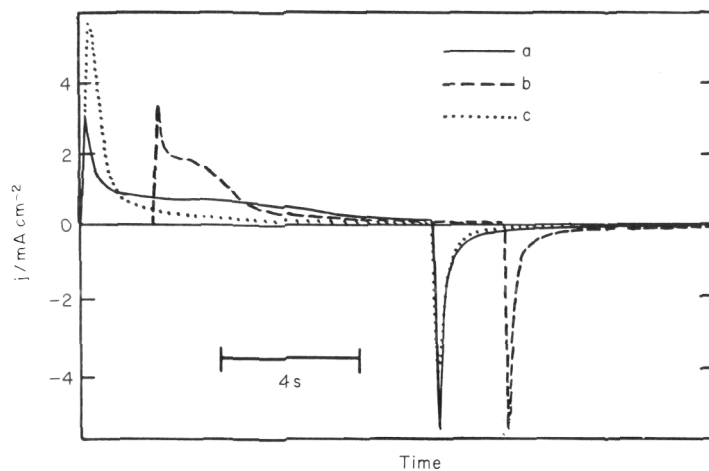


Fig. 6. $j-t$ response to the potential step to $E_+ = 1.35$ V from (a) $E_- = 0$ V, (b) 0.5 V and (c) 1.0 V.

result is consistent with the symmetrical appearance of the CV when the lower limit is increased to ca. 1.2 V or more (Fig. 2).

The influence of the potential pulse width on the $j-t$ response showed that, the longer the time at E_- , the lower and broader the current maximum, similar to the effect seen by extending E_- negatively. This can again be explained in terms of more complete film reduction, with associated diminished ion and solvent content, and thus a higher film resistance. This effect can also be demonstrated by the

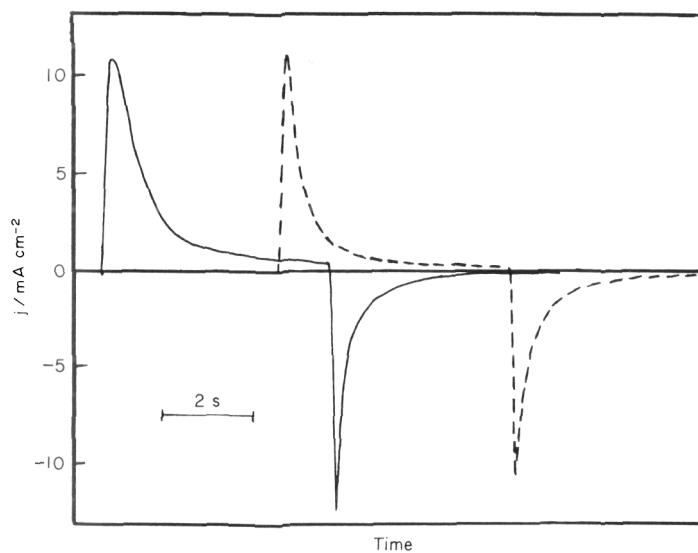


Fig. 7. $j-t$ response of oxide film to 5 s pulses to 1.37 V from 1.0 V (—) and 1.28 V (- -).

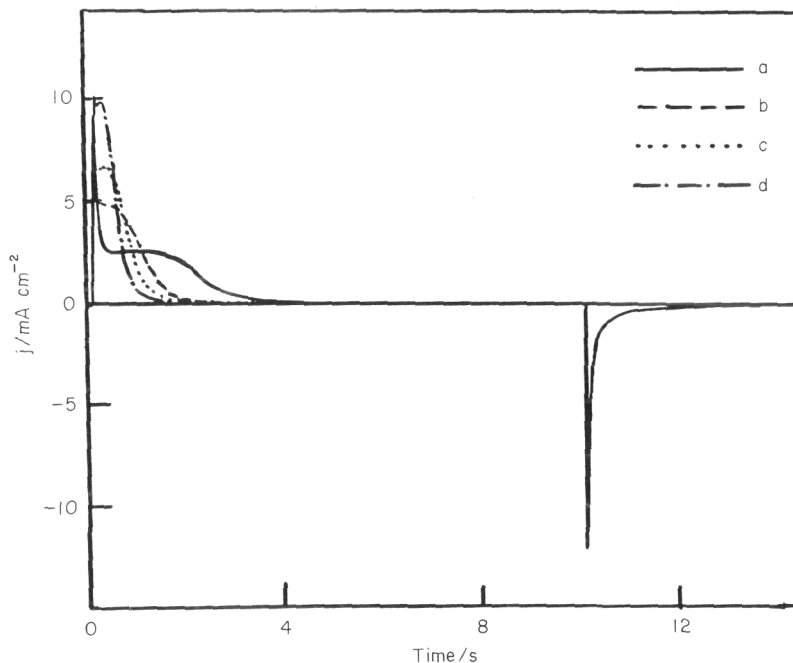


Fig. 8. Transient response of oxide subjected to 10 s pulses from 1.4 to 1.0 V after 5 min at 1.0 V. Successive pulses labeled a to d.

application of repeated pulses from, for example, 1.0 V to 1.4 V (Fig. 8), after several minutes spent at 1.0 V. It can be seen that the shape of the anodic transient becomes sharper with time, and that the maximum gradually disappears as insufficient time is available for complete film reduction. Finally, the presence of the current maximum is more pronounced for thicker oxide films.

Diffusion coefficient determination

To compare the apparent diffusion coefficient obtained from chronoamperometry with that determined from the CV data, the $j-t$ transients were analyzed in terms of the Cottrell equation

$$j = nFcD^{1/2}/(\pi t)^{1/2} \quad (2)$$

where c is the concentration of active sites in the film, D is the apparent diffusion coefficient and n , the number of electrons passed per electroactive center, is assumed to be unity. c can be estimated from

$$c = Q/nFV \quad (3)$$

where Q is the charge passed in peaks A_2/C_2 in a slow sweep experiment, when all the sites have reacted, and V is the film volume, determined from the area of

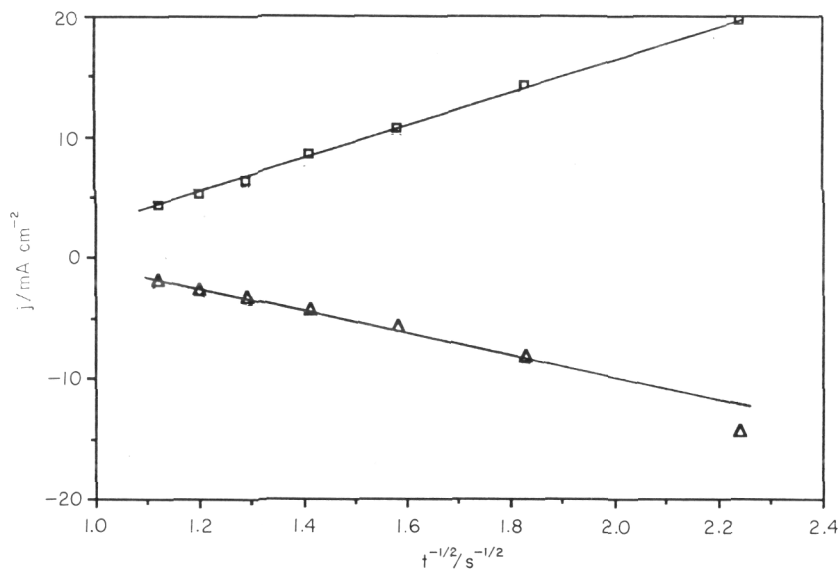


Fig. 9. Cottrell plots for oxide film subjected to successive potential pulses between 1.0 and 1.45 V.

the electrode and the (dry) film thickness determined from scanning electron microscope (SEM) investigations [6].

Figure 9 shows both anodic and cathodic $j-t^{1/2}$ plots for a number of experimental conditions. These plots do not go through the origin, which may be indicative of resistive effects at short times [8]. However, even with the use of IR compensation, these nonzero intercepts are still present, and therefore either the IR compensation is inadequate when the resistance of the system changes over the course of the oxidation-reduction process, or this effect has another origin.

From the linear part of the slope of these plots, $D \approx 2.4 \times 10^{-10} \text{ cm}^2 \text{ s}^{-1}$ for the negative step, very similar to that obtained from the analysis of the CV data. The slope obtained for the anodic $j-t^{1/2}$ data led to a value of $1.9 \times 10^{-10} \text{ cm}^2 \text{ s}^{-1}$.

Anomalous charge ratios – oxide disproportionation

As referred to earlier, and seen from Figs. 5, 6 and 8, the ratio of the anodic to cathodic charge density during potential pulsing is usually greater than, and can be up to ca. 4. This is particularly true when E_+ is in the range which yields the current maximum, i.e. ca. 1.35–1.45 V, the more negative E_- is and the thicker the oxide film. This is shown clearly in Fig. 10 in a plot of the charge ratio versus E_+ for a number of different experimental conditions.

It is very important to note that the same unusual charge ratios continue to be observed even after many identical potential pulses are applied and are independent of IR compensation. Furthermore, the anodic charge density never exceeds

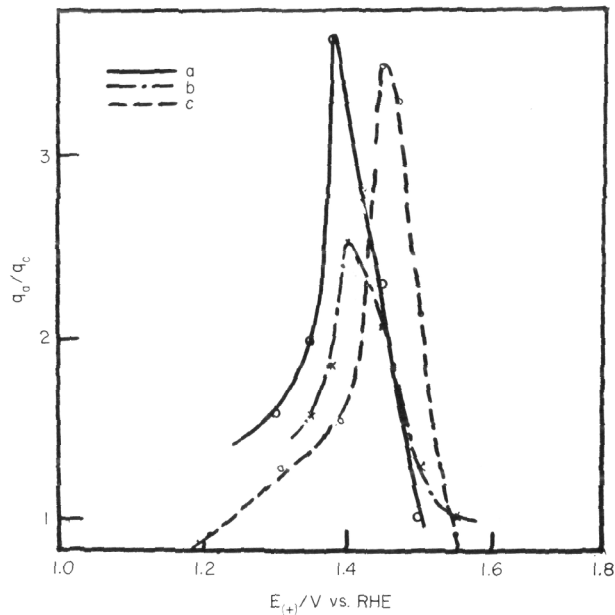


Fig. 10. Dependence of anodic-to-cathodic charge ratios on E_+ for oxide films of varying thickness: (a) 250 Å and (b) 100 Å at $E_- = 1.0$ V; (c) 300 Å at $E_- = 0$ V.

that observed in a slow sweep CV experiment, remaining virtually constant in repeat experiments. Therefore these results rule out the occurrence of other oxidation reactions such as the OER or metal/oxide dissolution during the positive step.

In order to investigate these effects further, a combination of chronoamperometry and voltammetry was used. In Fig. 11 (curve a), the potential was scanned to 1.45 from 1.00 V at 100 mV s^{-1} , but stepped negatively, resulting in an unusual charge ratio of ca. 3. When the potential was stepped between these limits (curve b), the ratio is now ca. 2. When the potential was stepped positively, but scanned negatively, the cathodic charge increased and the charge ratio is close to unity (curve c). These results demonstrate very clearly that there is no loss of charge in the positive pulse, but that the oxide reduction charge is anomalously low when a negative potential step is employed.

In another series of experiments (not shown in the figure), the potential was stepped positively but scanned negatively at different sweep rates. At sweep rates less than ca. 500 mV s^{-1} , q_a/q_c is close to unity. q_c then decreases significantly when the negative sweep rate is increased beyond this, while q_a remains constant.

On the basis of the above, it is suggested that, during the negative pulse, the oxide film is reduced both electrochemically, as monitored by the charge which passes, and in a parallel chemical reaction. As this occurs only when the potential

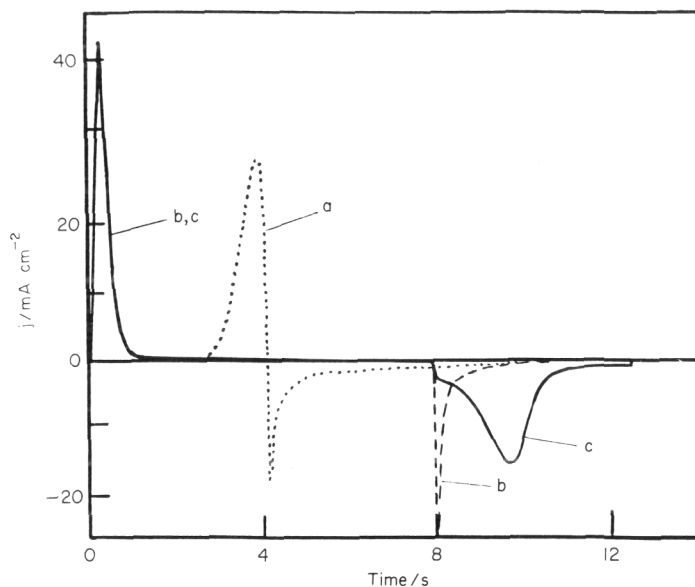


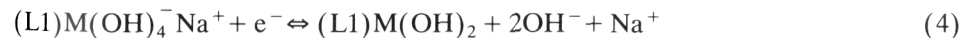
Fig. 11. Combination of potential scan and step experiments ($E_+ = 1.45$ V; $E_- = 0.98$ V; $s = 100$ mV s $^{-1}$): (a) positive sweep, negative step; (b) positive step, negative step; (c) positive step, negative sweep.

is decreased rapidly, it is also proposed that this is a result of nonequilibrium conditions which are generated within the oxide film.

Examination of reaction (1) shows that, during oxide reduction, both OH^- and Na^+ ions should be expelled from the oxide film. Assuming, first, that the diffusion-controlled behavior observed in Fig. 4 reflects slow electron hopping through the oxide film, then film reduction can be envisaged as commencing at the metal-oxide interface and proceeding, with time, towards the solution.

To simplify this discussion, the oxide film can be considered as a series of plates lying parallel to the electrode surface, each of which may contain numerous monolayers of oxide (Fig. 12). For the purpose of this discussion, the oxide is assumed to be in the M^{III} state at E_+ and the M^{II} state at E_- , where M represents the electroactive metal center. At E_+ the oxide is considered to be saturated with the required ions and solvent. When the anodic current decays to zero, it is assumed that all sites have been converted to the M^{III} state.

When E_- is applied, electrons are injected into the film, reducing the M^{III} sites in layer 1 (Fig. 12), denoted in the reactions below as L1 [32]:



The OH^- (and Na^+) species generated will then diffuse towards the outer solution. With time at E_- , electrons will be continuously injected into the film, gradually reducing the outer layers. During this process, as OH^- moves outwards, a pH gradient will develop across the film such that the pH is higher further

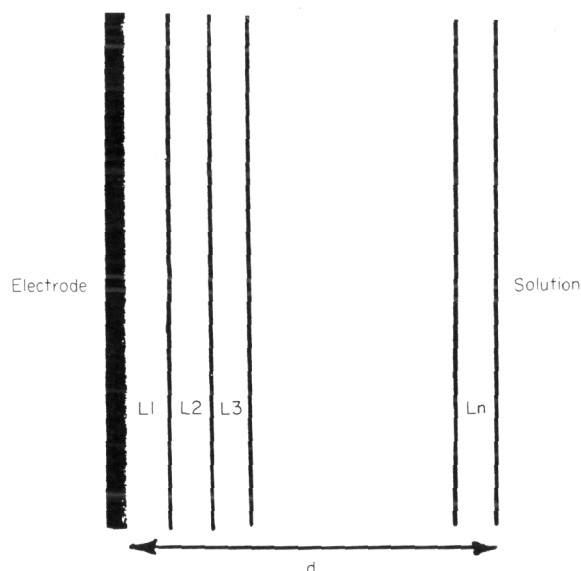
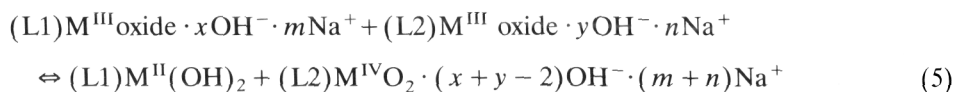


Fig. 12. Schematic diagram of hydrous Ni+Co oxide film, using the labeling system described in the text.

outwards and lower towards the inner portions of the oxide film. Under these conditions, adjacent layers of film in the M^{III} state could form a "concentration cell". The M^{III} sites at lower pH will oxidize nearby M^{III} sites at higher pH, leading to the following type of redox reaction:



The MO_2 generated at this potential (e.g. NiO_2 and/or CoO_2) is not expected to be stable [36,37] in this potential range, and has been reported to disproportionate rapidly to oxygen and M^{II} oxide [37]. In this manner, some M^{III} oxide is reduced to M^{II} oxide without the passage of an electron into the underlying metal, leading to lower measured cathodic versus anodic charge densities.

It should be noted that if the rate of reduction of these Ni + Co oxides were controlled by ion diffusion, then the reaction would commence at the outer film-solution interface. Again, a pH gradient could be established within the film, but would encompass the reduced M^{II} sites, i.e. the ionic gradient would lag behind the reaction front. These M^{II} sites would not be readily converted to a stable lower oxidation state at E_+ . Ni^{II} oxide, in particular, can be reduced only to metallic Ni, and only at potentials less than ca. 0.0 V.

It is also possible that, during the potential step to E_- , a high local pH is generated in the reacting part of the film. This could shift the local M^{III} - M^{IV} equilibrium potential negatively, so that some oxidation of the M^{III} sites occurs

during the cathodic pulse. As the pH stabilizes, the newly formed M^{IV} oxide could again disproportionate to form M^{II} oxide and oxygen, which would lead to the lower measured cathodic charge.

During the oxidation step, if electron hopping is the rate-determining step, the reaction would commence at the metal-oxide interface. As hydroxide ions are injected into the oxide film, the pH gradient would exist in the reduced (outer) part of the film and no disproportionation could then occur. If ion diffusion were rate determining during film oxidation, then the pH gradient would develop in the outer part of the film and would then encompass the oxidized region, so that disproportionation could once again take place. This would lead to an increase in the measured anodic charge density at high rates of oxidation versus that at slower rates. As the anodic charge is found to be independent of the rate of oxidation, it is probable that electron hopping is also rate limiting during oxidation.

SUMMARY

Oxide films, formed at an amorphous Ni + Co-based alloy electrode by a continuous potential cycling method, display an asymmetrical CV response similar to many polymer-coated electrode systems. The principal anodic peak exhibits a strong dependence on a number of experimental variables, shifting positively and narrowing as the lower potential limit is made more negative and when longer times are spent at this potential. The cathodic peak is always substantially broader than the anodic one and is independent of the above variables, and can therefore be studied kinetically. Films having a thickness greater than several hundred ångströms show diffusion-controlled behavior at standard sweep rates with a diffusion coefficient, during reduction, of ca. $2 \times 10^{-10} \text{ cm}^2 \text{ s}^{-1}$. The overall nature of the CV response and the magnitude of the cathodic diffusion coefficient, as compared with those of polymer films at electrodes, may indicate that the oxide film expands during oxidation by the injection of ions and associated solvent, and contracts during reduction.

Under potential step conditions, anodic transients show unusual maxima which are more pronounced at more negative and longer times at the lower limit, for thicker films and at particular upper potential limits. The cathodic $j-t$ response is exponential in nature, yielding a diffusion coefficient of similar magnitude to that obtained from sweep experiments. Under most conditions, the cathodic transient involves significantly less charge than during the oxidation step. This is hypothesized to reflect the occurrence of a disproportionation reaction between the oxidized sites, brought about by the establishment of local concentration cells induced by pH gradients under non-steady-state conditions within the oxide film.

ACKNOWLEDGEMENT

Support of this work by the Natural Sciences and Engineering Research Council of Canada is gratefully acknowledged.

REFERENCES

- 1 L.D. Burke and T.A.M. Twomey, *J. Electroanal. Chem.*, 167 (1984) 285.
- 2 L.D. Burke and D.P. Whelan, *J. Electroanal. Chem.*, 109 (1980) 385.
- 3 D.N. Buckley and L.D. Burke, *J. Chem. Soc. Faraday Trans. I*, 71 (1975) 1447.
- 4 L.D. Burke and E.J.M. O'Sullivan, *J. Electroanal. Chem.*, 93 (1978) 11.
- 5 L.D. Burke and E.J.M. O'Sullivan, *J. Electroanal. Chem.*, 117 (1981) 155.
- 6 K. Lian and V.I. Birss, *J. Electrochem. Soc.*, under review.
- 7 K. Lian and V.I. Birss, *J. Electrochem. Soc.* under review.
- 8 P. Daum and R.W. Murray, *J. Phys. Chem.*, 89 (1981) 389.
- 9 P.J. Peerce and A.J. Bard, *J. Electroanal. Chem.*, 114 (1980) 89.
- 10 P. Daum and R.W. Murray, *J. Electroanal. Chem.*, 103 (1979) 289.
- 11 A.H. Schroeder, F.B. Kaufman, V. Patel and E.M. Engler, *J. Electroanal. Chem.*, 113 (1980) 193.
- 12 A.H. Schroeder and F.B. Kaufman, *J. Electroanal. Chem.*, 113 (1980) 209.
- 13 F.B. Kaufman and E.M. Engler, *J. Am. Chem. Soc.*, 10 (1979) 547.
- 14 F.B. Kaufman, A.H. Schroeder, E.M. Engler, S.R. Kramer and J.Q. Chambers, *J. Am. Chem. Soc.*, 192 (1980) 483.
- 15 D. Orata and D.A. Buttry, *J. Am. Chem. Soc.*, 109 (1987) 3574.
- 16 P.G. Pickup and V.I. Birss, *J. Electroanal. Chem.*, 220 (1987) 83.
- 17 P.G. Pickup and V.I. Birss, *J. Electroanal. Chem.*, 240 (1988) 171.
- 18 L.D. Burke and T.A.M. Twomey, *J. Electroanal. Chem.*, 162 (1984) 101.
- 19 P.G. Pickup and V.I. Birss, *J. Electrochem. Soc.*, 135 (1988) 127.
- 20 P.G. Pickup and V.I. Birss, *J. Electroanal. Chem.*, 240 (1988) 185.
- 21 L.D. Burke and E.J.M. O'Sullivan, *J. Electroanal. Chem.*, 93 (1978) 11.
- 22 L.D. Burke, T.A.M. Twomey and D.P. Whelan, *J. Electroanal. Chem.*, 107 (1980) 201.
- 23 L.D. Burke and T.A.M. Twomey, *J. Electroanal. Chem.*, 134 (1982) 353.
- 24 V. Birss, R. Myers, H. Angerstein-Kozłowska and B.E. Conway, *J. Electrochem. Soc.*, 131 (1984) 1502.
- 25 H. Angerstein-Kozłowska, J. Klinger and B.E. Conway, *J. Electroanal. Chem.*, 75 (1977) 45.
- 26 C.R. Martin, I. Rubinstein and A.J. Bard, *J. Am. Chem. Soc.*, 104 (1982) 4817.
- 27 G. Inzelt, J.Q. Chambers, J.F. Kinstle and R.W. Day, *J. Am. Chem. Soc.*, 106 (1984) 3396.
- 28 D.A. Buttry and F.C. Anson, *J. Am. Chem. Soc.*, 104 (1982) 4824.
- 29 N. Oyama and F.C. Anson, *J. Electrochem. Soc.*, 127 (1980) 640.
- 30 A.J. Bard and L.R. Faulkner, *Electrochemical Methods*, Wiley, Toronto, 1980, p. 143.
- 31 D.M. MacArthur, *J. Electrochem. Soc.*, 117 (6) (1970) 729.
- 32 K. Lian, M.Sc. Thesis, University of Calgary, 1988.
- 33 M.R. Tarasevich and B.N. Efmov, in S. Trasatti (Ed.), *Electrodes of Conductive Metallic Oxides*, Elsevier, New York, 1980.
- 34 V.I. Birss and M.T. Shevalier, *J. Electrochem. Soc.*, 134 (1987) 1594.
- 35 J.A. Garrido, F. Centellas, P.L. Cabot, R.M. Rodríguez and E. Perez, *J. Appl. Electrochem.*, 17 (1987) 1093.
- 36 M. Pourbaix, *Atlas of Electrochemical Equilibria in Aqueous Solutions*, 2nd English ed. NACE, Houston, TX, 1974.
- 37 P. Rasiyah and A.C.C. Tseung, *J. Electrochem. Soc.*, 129 (1982) 1724.